# Longitudinal Motion Control of Underactuated Cruising AUVs for Acoustic Bottom Survey

Kangsoo Kim [a]

*National Maritime Research Institute, National Institute of Maritime, Port and Aviation Technology,*
*6-38-1 Shinkawa, Mitaka, Tokyo 181-0004, Japan*

Keywords: Longitudinal Motion Control, Acoustic Bottom Survey, Cruising AUV, Underactuated, Depth Control, Bottom Following.

Abstract: Longitudinal motion control approaches for underactuated cruising AUVs primarily tasked with acoustic bottom surveys are addressed. For controlling the longitudinal motion of a cruising AUV, we implemented waypoint-based depth control and terrain following approaches during simulated acoustic bottom survey missions. Simulation results revealed that the distinct motion control approaches significantly influence the pitch motion of the vehicle, thereby directly impacting the quality of the acoustic bottom survey results. The safety issue of a cruising AUV, particularly regarding the occurrence of bottom collisions during its near-bottom survey missions is also investigated in this research. Concerning the safety issue, we found that while traversing the same trackline, the likelihood of an AUV encountering a bottom collision varies considerably, based on the specific motion control approach being utilized.

## 1 INTRODUCTION

Conducting high-definition bottom surveys is a pivotal task encompassing a diverse range of ocean development endeavours, with particular significance in the exploration of submerged natural resources like marine minerals, offshore oil, and gas. Preceding the essential bottom samplings in the conclusive phase of surveys targeting these resources, a high-definition bottom mapping or imaging is imperative. In the realm of underwater exploration of such purposes, the Autonomous Underwater Vehicle (AUV) assumes a vital role. It facilitates the acquisition of bottom survey data with considerably higher definition compared to what can be obtained through surface vessels (Honsho et al., 2015; 2016). In regard to acoustic bottom surveys, nowadays, bottom mapping sonars like Multi-Beam Echo Sounder (MBES) or Interferometry Sonar (IFS) have achieved widespread utilization in AUV-based high-definition seabed surveys (Ferrini et al., 2007; Kim et al., 2023). In the context of acoustic bottom mapping, it is widely recognized that the angular motion of a mapping sonar typically has a significant impact on the accuracy of mapping results. More specifically, it is well known that excessive pitch or roll motion significantly degrades the quality of acoustic bottom mapping (Cobra et al., 1992; Kim et al., 2023).

Based on their behavioural characteristics, AUVs are typically categorized into two groups: cruising or flight-class AUVs, and hovering AUVs (Lea et al., 1999; Houts et al., 2012). While a hovering AUV has the capability to remain stationary and manoeuvre around a specific operational point, the majority of cruising AUVs lack this ability. This arises from the fact that the majority of cruising AUVs are underactuated, which means they possess fewer actuators than the degrees of freedom (DOF) they need to control (Spong, 1998; Tedrake, 2009). Underactuation results in certain degrees of freedom becoming uncontrollable, thereby limiting the path-following capability of underactuated systems. Hence, it is easy to envision that a cruising AUV inherently faces challenges when it comes to evading imminent collisions with nearby obstacles (Pedbody, 2008; Kim et al. 2023). In terms of the vehicle dynamics, the underactuation presents itself as the coupled vehicle motion. Within the framework of the longitudinal dynamics of a cruising AUV, for example, heave and pitch motions are strongly

[a] https://orcid.org/0000-0003-1496-4145

coupled. Consequently, whenever a cruising AUV alters its vertical position, a concurrent pitch motion invariably accompanies. In case a cruising AUV flies over a flat and uniform seafloor without a specific objective, it does not need to alter its vertical position with respect to the surface, that is, its depth. In general, however, similar to terrestrial landscapes, there are various complex bathymetric features consisting of submarine valleys and mountains on the seafloor as well. This implies that a cruising AUV engaged in its bottom survey mission must consistently adjust its vertical position, leading to continuous changes in its pitch motion. It is readily foreseeable that as an output of a closed-loop control system, the pitch motion response of a cruising AUV is directly influenced by the approach taken to control the longitudinal motion of it. And in general, it can be asserted that the most suitable longitudinal motion control for AUV-based acoustic bottom survey is achieved by minimal alterations in pitch motion. On the flip side, the longitudinal motion control of an AUV significantly influences vehicle safety, as it shapes the vertical flight trajectory that directly impacts the likelihood of the AUV encountering a bottom collision. Therefore, it is apparent that determining an approach for the longitudinal motion control of a cruising AUV during an acoustic bottom survey has to take into account both safety concerns and the minimization of pitch motion. In this research, we conducted a simulation-based investigation to analyse the characteristics of some waypoint-based longitudinal motion control approaches. Based on the investigation results, we found that the probability of an AUV encountering a bottom collision varies significantly while traversing the same trackline, depending on the particular motion control approach being employed.

# 2 LONGITUDINAL MOTION CONTROL

The longitudinal motion control of a cruising AUV involves motion adjustments within the vertical plane, in order to ensure precise vertical motion of it. In the majority of cases, the controlled variable for the longitudinal motion control of an AUV is either the depth beneath the surface or the altitude above the seabed (Caccia et al., 2003). It is noted that the motion control of an AUV achieved through seabed-based altitude control using a fixed reference is referred to as terrain following (Hérissé et. al, 2010; McPhail et. al, 2010) or bottom following (Bennet et al., 1995;

Caccia et. al, 1999). Therefore, while conducting a terrain-following flight, an underwater vehicle is managed to consistently maintain a specific altitude above the along-track bottom surface. On the other hand, depth control uses the depth beneath the surface as a reference for position control within the vertical plane.

## 2.1 Waypoint-Based Navigation

The navigation systems employed in the majority of present-day AUVs for commercial, civilian, and military applications predominantly depend on predetermined nominal tracklines, which are composed of waypoints defined within the earth-fixed frame (Figure 1).
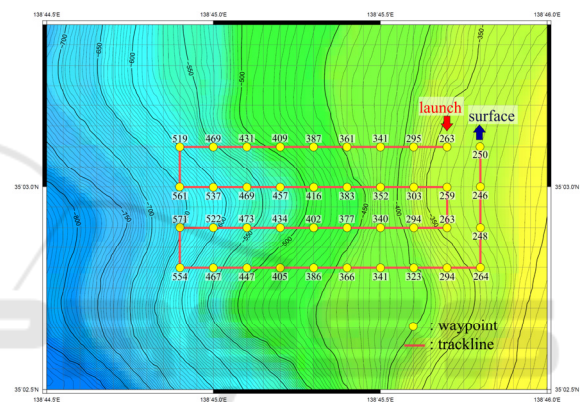


Figure 1: Waypoints and corresponding nominal tracklines established for an AUV mission.

In Figure 1, each waypoint is labelled with a number that corresponds to the assigned reference depth. That is, during the mission as depicted in Figure 1, the longitudinal motion of an AUV is controlled to track the reference depths in a sequential manner. It is noted here that, in the context of waypoint-based navigation, when a vehicle approaches the vicinity of the current target waypoint within a predefined acceptable range, the target waypoint is updated to the subsequent one (Medagoda and Gibbens, 2010). Therefore, in our waypoint-based AUV navigation implemented by depth control, no sooner has the vehicle reached *(n-1)*-th waypoint, i.e., *wp_n-1*, then the reference depth of *(n)*-th waypoint is activated, deactivating that of current *(n-1)*-th waypoint simultaneously (Figure 2a). This waypoint activation rule is also extended to the longitudinal motion control of other control outputs. In case of altitude control, a reference altitude is assigned to a waypoint, making an AUV engage in terrain-following flight until it reaches that waypoint. In Figure 2b, a terrain-

following flight of an AUV implemented on the basis of the waypoint-based navigation is depicted.
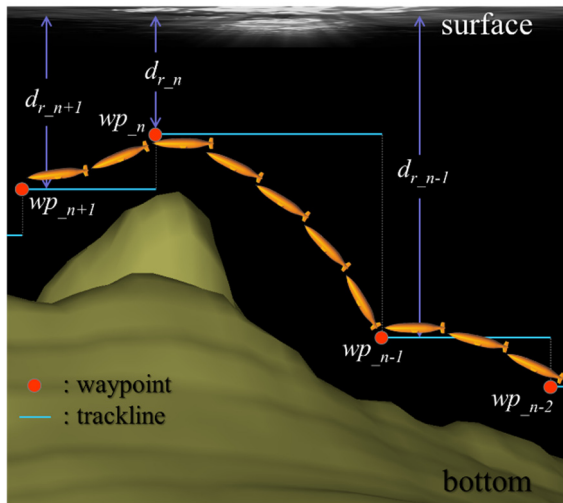


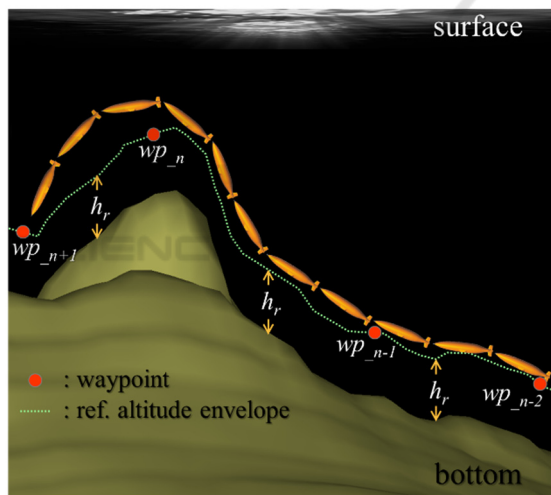Figure 2a: Waypoint-based AUV navigation implemented by depth control.



Figure 2b: Waypoint-based AUV navigation implemented by altitude control.

In Figure 2a, $d_{r\_n}$ represents the reference depth assigned to the *(n)*-th waypoint, while in Figure 2b, $h_r$ represents the reference altitude assigned to all waypoints for the terrain-following flight of an AUV.

Altitude control operates by utilizing the altitude error, which is defined as the disparity between a vehicle's current altitude and the designated reference altitude.

It is worth noting that by substituting the altitude error with its corresponding depth error, a depth controller can effectively facilitate altitude control as well (McPhail et al., 2010; Kim and Ura, 2015). In

such cases, we see that within the along-track interval spanning from the *(n-1)*-th to the *(n)*-th waypoint, altitude control is executed through the use of the depth error, as shown in (1).

$$e_d = -e_h = h - h_r \qquad (1)$$

In (1), $e_d$ and $e_h$ respectively denote the depth error and altitude error, while $h$ denotes the current vehicle altitude.

## 2.2 Underactuation and Pitch Motion

As previously mentioned, cruising AUVs inherently exhibit underactuation. Owing to the emphasis on highly efficient cruising performance, cruising AUVs feature a slender body shape. Like turning and pull-ups, cruising AUVs alter their course by changing their orientation, effectively changing their direction of movement through manoeuvrers. This appears in the form of the coupling in vehicle motion, that is, the surge-heave-pitch coupling in longitudinal dynamics, and sway-roll-yaw coupling in lateral dynamics of the vehicle motion. It is well known that within the framework of the longitudinal dynamics of a cruising AUV, heave-pitch coupling is particularly strong (McRuer et al., 1973; Kim and Ura, 2010). Hence, as depicted in Figure 2, whenever an underactuated vehicle adjusts its vertical position, corresponding changes in its pitch attitude invariably occur. Here comes the importance of selecting longitudinal motion control in acoustic bottom survey mission using a cruising AUV. As previously stated, the pitch motion directly influences the quality of the acoustic bottom survey.

## 2.3 Disruption in Acoustic Bottom Survey

As previously noted, contemporary AUV-based acoustic bottom surveys extensively utilize advanced bottom mapping sonars like MBES or IFS. Using a wide acoustic fan-shaped pulse, a bottom mapping sonar necessitates precise tracking of its angular movement to ascertain the transmission and reception angles for each individual beam. Hence, the absence of the proper attitude compensation for the platform carrying the sonar prevents accurate echo sounding through a bottom mapping system. In contemporary bottom mapping sonar systems, real-time attitude data sourced from navigation devices like an Inertial Navigation System (INS) or an Attitude Heading Reference System (AHRS) are commonly employed for this purpose. However, there exists a limitation on the attitude that can be compensated for in echo

sounding. Figure 3 shows a result of acoustic bottom mapping obtained by a near-bottom survey using a cruising AUV. For the bottom mapping, a MBES system working at 400 kHz was used.
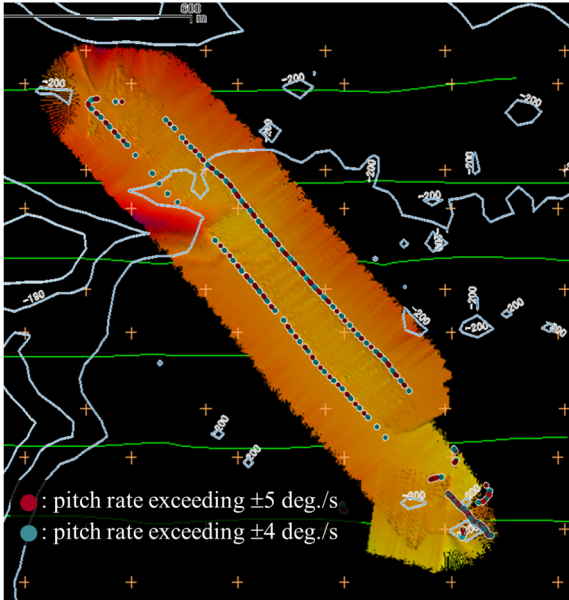


Figure 3: A result of acoustic bottom mapping with highlighted excessive along-track pitch rates.

As seen in the figure, the resulting bottom bathymetry exhibits pronounced undulations in the along-track direction, which are scarcely representative of real-world bathymetric features. In Figure 3, along-track pitch rates exceeding ±4 deg., a magnitude too substantial to be adequately compensated for by a typical bottom mapping sonar (Teledyne Reason, 2012), are overlaid onto the bottom bathymetry map. As seen in the figure, the pronounced undulations exhibit a strong correlation with the highlighted along-track points, showing the prominent impact of excessive pitch rates on the bottom mapping.

# 3 HARDWARE SYSTEM AND GNC ARCHITECTURE

## 3.1 Hardware System

While the AUV navigation strategy outlined in this paper holds a general-purpose nature, its initial implementation was conducted on the hardware system of our cruising AUV, referred to as NMRI C-AUV#04. As the latest model of our cruising AUVs, NMRI C-AUV#04 was designed and developed by National Maritime Research Institute (NMRI) of

Japan. With the aim of achieving a highly-efficient near-bottom survey over challenging steep terrains, the NMRI C-AUV#04 prioritized the core features encompassing exceptional high-manoeuvrability and high-speed capability. As a result, accompanied by an adjustable pitch range of ±80 deg., the NMRI C-AUV#04 attains the maximum velocity of 3.3 m/s. Figure 4 depicts the overall layout of the NMRI C-AUV#04. And in Table 1, principal dimensions and main specifications of the vehicle are listed.
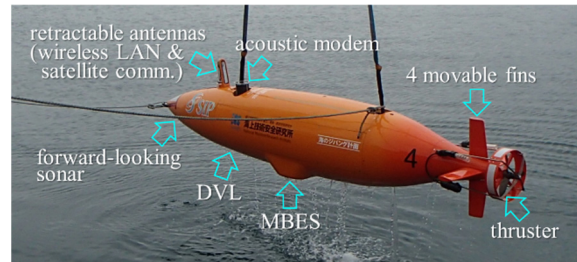


Figure 4: Overall layout of NMRI C-AUV#04.

Table 1: Principal dimensions and vehicle specifications of NMRI C-AUV#04.

| Principal dimensions | |
|---|---|
| Length overall | 3.9 m |
| Diameter | 0.65 m |
| **Main specifications** | |
| Mass | 545 kg |
| Speed (designed / max.) | 1.8 / 3.3 m/s |
| Depth rating | 2000 m |
| Controllable pitch | ±80 deg. |
| Endurance | 19 hrs. @ 1.8 m/s |

## 3.2 GNC Architecture

Within our vehicle system, it is worth noting that we utilize a Guidance, Navigation, and Control (GNC) architecture that rests upon a hierarchical control structure encompassing two distinct control levels. Namely, this encompasses high-level control for guidance and navigation, alongside low-level control dedicated solely to tracking, as illustrated in Figure 5.
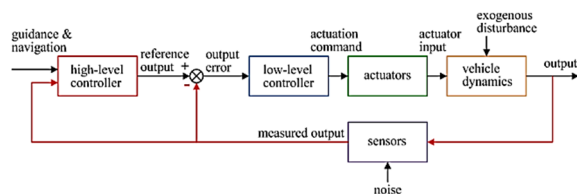


Figure 5: GNC architecture composed of two-level hierarchical control.

Generally, in the longitudinal dynamics of a cruising AUV, akin to aircraft, the primary outputs encompass surge, heave, and pitch. On the lateral axis, the counterparts consist of sway, roll, and yaw (McRuer et al., 1973). Following the prevalent model of bifurcated vehicle dynamics commonly applied in flight control, our GNC system incorporates two distinct feedback controls at the lower level: one for depth (altitude) to manage longitudinal dynamics, and the other for heading to govern lateral dynamics. Figure 6 shows the schematic of the depth control implemented in our vehicle system (Kim and Ura, 2009). As depicted in the figure, our depth control consists of dual feedback loops. While the outer loop governs depth control, it utilizes the depth error to derive a proportional pitch reference, within which the nested pitch-to-elevator control operates. Hence, throughout our depth control process, the pitch control operates implicitly and continuously.
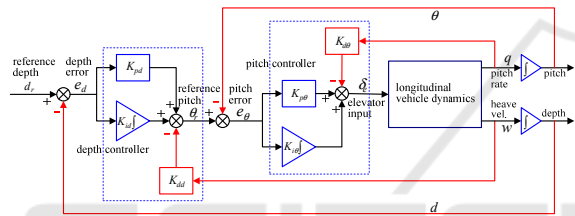


Figure 6: Schematic of the depth (altitude) control architecture of a cruising AUV.

## 4 SIMULATIONS

### 4.1 Conditions for Simulations

Figure 7 shows a 2D top view of the waypoints and trackline superimposed onto the bathymetric map, employed in our simulations.
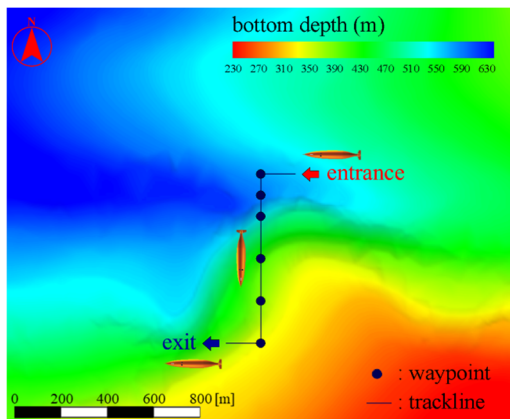


Figure 7: Top view of the terrain, waypoints, and trackline employed in simulations.

The digital bathymetric map data has been sourced from the bottom bathymetry database situated in Suruga Bay, located in Shizuoka Prefecture, Japan. Running southward, the trackline crosses the site's steepest terrain, where the maximum along-track slope angle exceeds 40 degrees.

In this research, we have affirmed the suitability of longitudinal motion control approaches for acoustic bottom surveys by conducting simulations utilizing the mathematical model of the GNC system, in conjunction with the previously mentioned terrain data, waypoints, and trackline. The GNC system model comprises waypoint-based guidance, a low-level motion controller implemented through Proportional-Integral-Derivative (PID) compensation, and the vehicle dynamic model, as illustrated in Figure 6. Among these components, the dynamic model of NMRI C-AUV#04 has been derived through a system identification (SI) approach (Kim et al., 2023). In the array of models used to depict motion responses to actuator inputs, the pitch to elevator deflection transfer function is shown in (2).

$$\frac{q}{\delta_e} = \frac{-0.173s}{s^3 + 2.681s^2 + 0.546s + 0.048} \qquad (2)$$

In (2), $q$ is the pitch rate of the vehicle in deg./s, while $\delta_e$ is the elevator deflection in degree. As depicted in Figure 8, (2) accurately reproduces the vehicle's actual pitch response, resulting in a normalized root-mean-squared error (NRMSE) fitness of over 96%.
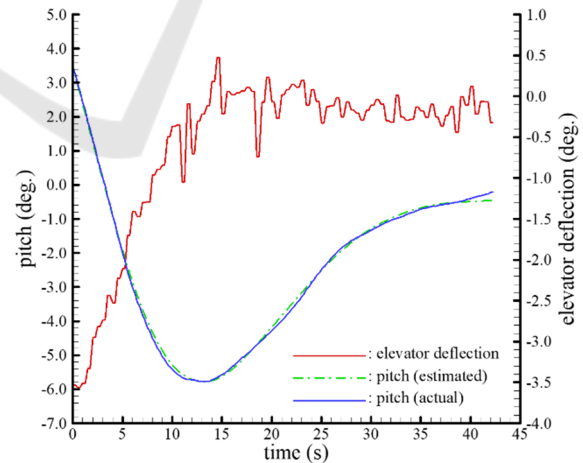


Figure 8: Estimated and actual pitch responses of NMRI C-AUV#04.

The state-space pitch dynamics of NMRI C-AUV#4 actually used in our time-domain simulation is shown in (3). Converted from the pitch to elevator deflection transfer function (2), (3) is a canonical form, the state

variables in which are directly related to the pitch response of the vehicle.

$$\dot{x}_q = A_q x_q + B_q u \tag{3a}$$

$$y_q = C_q x_q + D_q u \tag{3b}$$

In (3), $A_q$, $B_q$, $C_q$, $D_q$ are the state matrix, input matrix, output matrix, and feedforward matrix of the pitch dynamics of NMRI C-AUV#4 given by (4).

$$A_q = \begin{bmatrix} -2.681 & -0.546 & -0.192 \\ 1.0 & 0.0 & 0.0 \\ 0.0 & 0.25 & 0.0 \end{bmatrix} \tag{4a}$$

$$B_q = \begin{bmatrix} 0.5 \\ 0.0 \\ 0.0 \end{bmatrix} \tag{4b}$$

In (3), $x_q \in \mathbf{R}^3$ denotes the state vector. And as inferred from (2), the output vector $y_q$ corresponds to the pitch rate $q$, and the input vector $u$ represents the elevator deflection, denoted as $\delta_e$. It is important to mention here that in this paper, we consistently employ degree units for angular displacement and rate throughout.

## 4.2 Depth-Controlled Bottom Survey Flight

At first, we performed a simulation in which NMRI C-AUV#4 executes a depth-controlled bottom survey flight by following the waypoints shown in Figure 7. It is worth emphasizing that in this flight, the target altitude is set to be 80 m, with a minimum allowable altitude of 60 m. As a result, the along-track bottom section, elevated by 80 m, serves as the target altitude envelope. Figure 9 shows the 2D vehicle trajectory resulting from the simulation. 3D view of the same result is shown in Figure 10. As noted in the figures, depth control lets the vehicle successfully follow the waypoints.
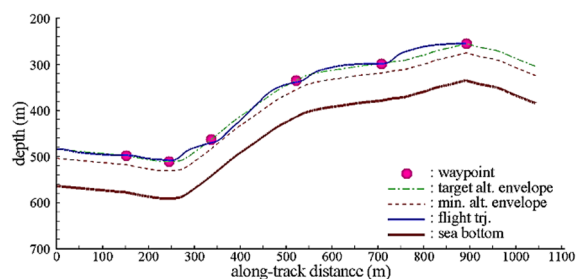


Figure 9: 2D view of simulated depth-controlled bottom survey flight.
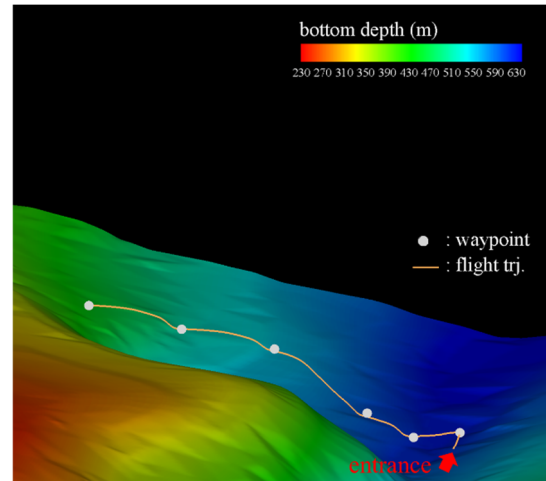


Figure 10: 3D view of simulated depth-controlled bottom survey flight.

Figure 11 depicts a comparison between the reference pitch and the simulated pitch response throughout the flight. The figure highlights excellent tracking performance in pitch control, a crucial factor in maintaining depth control performance. However, the substantial pitch amplitude, nearly reaching 48 degrees, is anticipated to adversely affect the results of the acoustic bottom mapping.
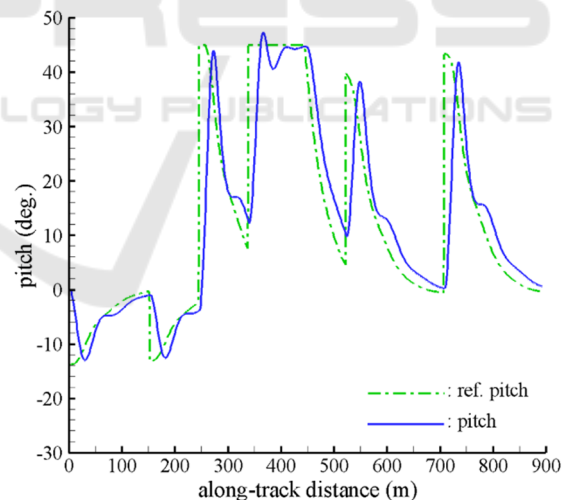


Figure 11: Pitch response during simulated depth-controlled bottom survey flight.

Simulated pitch rates are also shown in Figure 12. As seen in the figure, even the maximum peak value of pitch rates is below 5 deg./s. Moreover, the majority of pitch rates remain confined within the range of ±1 deg./s, a sufficiently small range to ensure stable bottom mapping (Teledyne Reason, 2012). Therefore, the pitch rate is thought to have limited adverse impact on the acoustic bottom survey.
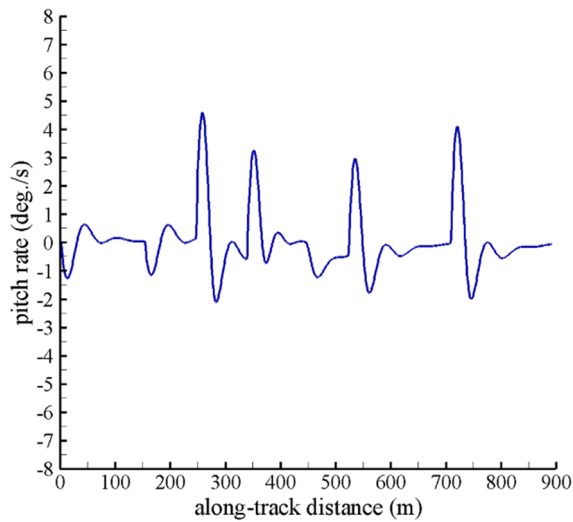
Figure 12: Pitch rate during simulated depth-controlled bottom survey flight.

In addition to the quality of acoustic bottom survey, safety concerns also play a crucial role in the evaluation of near-bottom flight for a cruising AUV. As previously discussed, the inherent underactuation of a cruising AUV poses a significantly greater risk of bottom collision when compared to fully-actuated underwater vehicles like hovering AUVs. Figure 13 depicts along-track vehicle altitudes that directly relate to the safety concerns associated with potential bottom collisions. As also noted in Figure 9, vehicle altitudes are consistently confined within a narrow range around the reference altitude of 80 m, ensuring they remain safely above the minimum allowable altitude of 60 m.
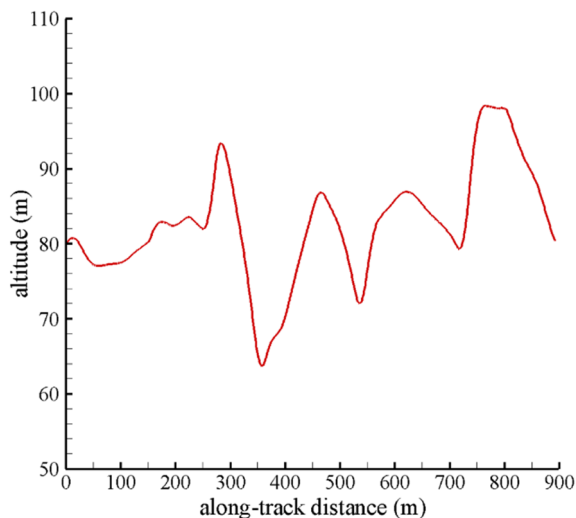


Figure 13: Vehicle altitude during simulated depth-controlled bottom survey flight.

## 4.3 Terrain-Following Bottom Survey Flight

Following the depth-controlled bottom survey flight, we then have simulated terrain-following flight. With the exception of the controlled output in longitudinal motion control of the vehicle, all simulation conditions remain identical to those employed in the previously depicted depth-controlled bottom survey flight. Figure 14 shows the 2D vehicle trajectory derived from the simulation. 3D view of the same result is depicted in Figure 15.
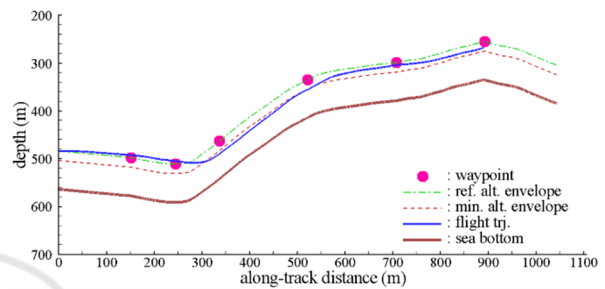


Figure 14: 2D view of simulated terrain-following bottom survey flight.
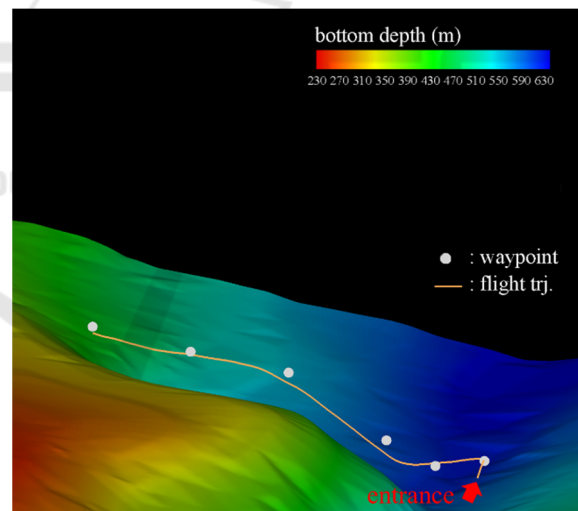


Figure 15: 3D view of simulated terrain-following bottom survey flight.

It is found that, overall, the flight trajectory exhibits a closer resemblance to the reference altitude envelope compared to that of the depth-controlled flight. And it is worth noting that while we are currently using the term reference altitude, we previously referred to it as target altitude for the depth-controlled flight. In depth control, the controlled output is the depth, not the altitude, which is why we employed the term target rather than reference.

In Figure 14, it is evident that while the flight trajectory closely resembles the reference altitude envelope, there are more or less discrepancies in their vertical positions. Moreover, in some tracks vertical positions of the vehicle fall below the minimum allowable altitude. This indicates significant safety concerns arising from the increased risk of potential collisions with the seafloor. A comparison between the reference pitch and the simulated pitch response throughout the flight is shown in Figure 16.
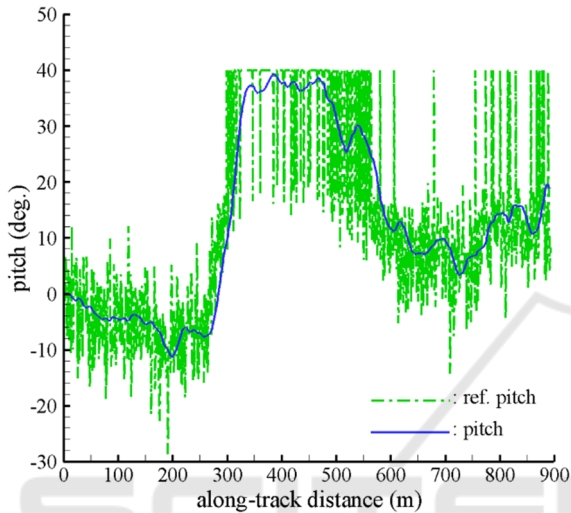


Figure 16: Pitch response during simulated terrain-following bottom survey flight.

Apparently, the pitch response obtained from the terrain-following flight is totally different from that of the depth-controlled flight. As observed in the figure, the reference pitch undergoes pronounced fluctuations throughout the flight. This is not particularly surprising, however, when considering the schematic of our altitude control architecture. As explained in 2.1 and 3.2, the pitch reference is derived through the PID compensation of the depth error, thus, for altitude control, the altitude error counterpart. Hence, during terrain-following flights, even minor alterations in the bottom elevation exert an influence on the reference pitch. It is worth noting here that in this simulation, the reference pitch is set to be restricted within the range of ±40 deg., as seen in Figure 16. Figure 17 shows simulated pitch rates. Despite the presence of high-frequency fluctuations, the magnitude of the pitch rate remains within a sufficiently narrow range. As seen in the figure, the majority of pitch rates are limited within the range of ±0.5 deg./s, which is half the range compared to that of the depth-controlled flight. Thus, in bottom-following flight, the pitch rate is unlikely to detrimentally impact acoustic bottom mapping.
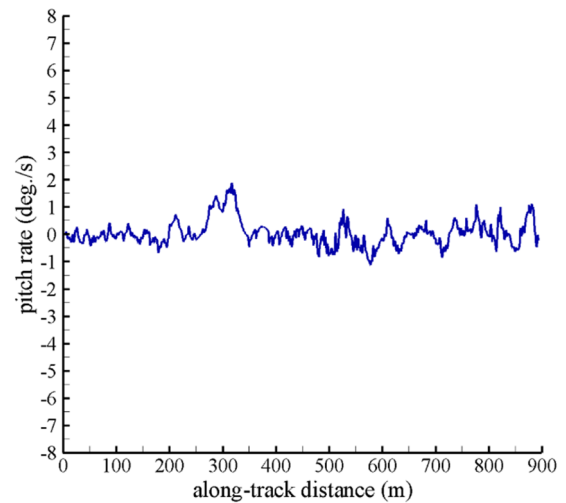


Figure 17: Pitch rate during simulated terrain-following bottom survey flight.

Along-track vehicle altitudes are shown in Figure 18. As previously mentioned and evident from Figures 14 and 18, in certain intervals, vertical positions of the vehicle fall below the minimum allowable altitude. Moreover, as observable in the figures, the majority of vehicle altitudes are below 80 m, the reference altitude for terrain-following flight. Thus, it can be said that from a safety perspective, the terrain-following flight result is not satisfactory.
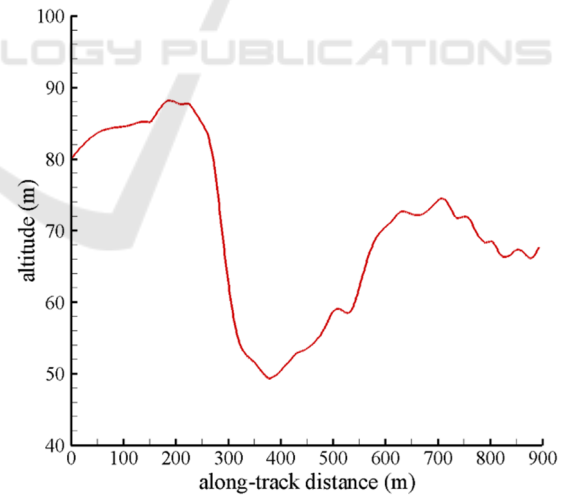


Figure 18: Vehicle altitude during simulated terrain-following bottom survey flight.

# 5 CONCLUSIONS

In order to clarify the impact of longitudinal motion control approaches on acoustic bottom surveys, we have conducted simulations of bottom survey flights.

The simulation results indicate that the depth-controlled bottom survey flight follows a trajectory at moderate altitudes well within an acceptable range. However, concerns arise regarding the potentially harmful impact on acoustic bottom mapping due to the pitch responses including some large amplitudes. On the other hand, while the magnitude of the pitch response is on a similar scale to that of depth control, the magnitude of the pitch rate is notably reduced by employing the terrain-following control approach. However, safety issues may arise during a terrain-following bottom survey flight. As a result of unsatisfactory bottom-following flight, including vertical vehicle positions below their allowable lower limit, the risk of potential collisions with the seabed can significantly increase. In conclusion, it is essential to exercise caution when selecting a type of longitudinal motion control. This decision should be made after careful consideration of various factors, such as the mission objectives, seafloor topography, target or reference altitudes, and vehicle dynamics, among others.

## ACKNOWLEDGEMENTS

## REFERENCES

Honsho, C., Ura, T., Asada, A., Kim, K., Nagahashi, K. (2015). High-resolution acoustic mapping to understand the ore deposit in the Bayonnaise knoll caldera, Izu-Ogasawara arc. *Journal of Geophysical Research: Solid Earth*, 120(4), 2169–9313.

Honsho, C., Ura, T., Kim, K., Asada, A. (2016). Postcaldera volcanism and hydrothermal activity revealed by autonomous underwater vehicle surveys in Myojin Knoll caldera, Izu-Ogasawara arc. *Journal of Geophysical Research: Solid Earth*, 121(6), 4085–4102.

Ferrini, V. L., Fornari D. J., Shank, T. M., Kinsey, J. C., Tivey M. A., Soule, S. A., Carbotte, S. M., Whitcomb, L. L., Yoerger, D., Howland J. (2007). Submeter bathymetric mapping of volcanic and hydrothermal features on the East Pacific Rise crest at 9°50'N. *Geochemistry, Geophysics, Geosystems*, 8(1), 1–33.

Kim, K., Sato, T., Oono, A. (2023). Depth-based pseudo-terrain-following navigation for cruising AUVs. *Control Engineering Practice*, 131(2023), article 105379, 10.1016/j.conengprac.2022.105379.

Cobra, D. T., Oppenheim, A. V., Jaffe, J. S. (1992). Geometric distortions in side-scan sonar images: a procedure for their estimation and correction. *IEEE Journal of Oceanic Engineering*, 17(3), 252–268.

Lea, R. K., Allen R., Merry S. L. (1999). A comparative study of control techniques for an underwater flight vehicle. *Int. J. of System Science*, 30(9), 947–964.

Houts, S. E., Rock, S. M., McEwen R. (2012). Aggressive terrain following for motion-constrained AUVs. In *IEEE/OES Autonomous Underwater Vehicles (AUVs)*. 1–7, Southampton.

Spong, M. W. (1998). Underactuated mechanical systems. In Siciliano B., Valavanis K. P. (Eds.) *Control Problems in Robotics and Automation.* Lecture Notes in Control and Information Sciences, 230, 135–150.

Tedrake, R. (2009). Underactuated robotics: Learning, planning, and control for efficient and agile machines: *Course Notes for MIT 6.832*. Working Draft Edition.

Pedbody, M. (2008). Autonomous underwater vehicle collision avoidance for under-ice exploration. *Journal of Engineering for the Maritime Environment*, 222(2), 53–66.

Caccia, M., Bruzzone, G., Veruggio, G. (2003). Bottom-following for remotely operated underwater vehicles: Algorithms and experiments. *Autonomous Robots*, 14, 17–32.

Hérissé B., Hamel T., Mahony R., Russoto, F.-X. (2010). A terrain-following control approach for a VTOL unmanned aerial vehicle using average optical flow. *Autonomous Robots*, 29, 381–399.

McPhail, S., Furlong, M., Pedbody, M. (2010). Low-altitude terrain following and collision avoidance in a flight-class autonomous underwater vehicle. *Journal of Engineering for the Maritime Environment*, 224(4), 279–292.

Bennet, A. A., Leonard, J. J., Bellingham, J. G. (1995). Bottom following for survey-class autonomous underwater vehicles. *9th International Symposium on Unmanned Untethered Submersible Technology*, 327–336, Durham.

Caccia, M., Bruzzone, G., Veruggio, G. (1999). Active sonar-based bottom-following for unmanned underwater vehicles. *Control Engineering Practice*, 7, 252–268.

Medagoda, E. D. B., Gibbens, P. W. (2010). Synthetic-waypoint guidance algorithm for following a desired flight trajectory. *Journal of Guidance, Control, and Dynamics*, 33(2), 601–606.

Kim, K., Ura, T. (2015). Longitudinal motion instability of a cruising AUV flying over a steep terrain, *IFAC-PapersOnline*, 48(2), 56–63.

McRuer, D., Ashkenas, I., Graham, D. (1973). *Aircraft Dynamics and Automatic Control*, Princeton University Press.

Kim, K., Ura, T. (2010). Applied model-based analysis and synthesis for the dynamics, guidance, and control of an autonomous undersea vehicle, *Mathematical Problems in Engineering*, 2010, article ID 149385.

Teledyne Reason (2012). *SeaBat 7125 AUV Operator's Manual*.

Kim, K., Ura, T. (2009). Optimal guidance for autonomous underwater vehicle navigation within undersea areas of current disturbances. *Advanced Robotics*, 23(5), 601–628.